Experiment study on friction drive

Guomin Wang*[ab], Lisheng Ma[a], Zhengqiu Yao[a], Guoping Li[a]
[a]National Astronomical Observatories/Nanjing Institute of Astronomical Optics & Technology, Chinese Academy Science, Nanjing 210042
[b]Graduate School of the Chinese Academy of Sciences, Beijing 100039

ABSTRACT

In the past years, friction drive was developed to overcome the inherent deficiencies in both worm drive and gear drive. No periodical error and free of backlash are the main advantages of friction drive. With the trend towards bigger and bigger aperture of the optical telescopes, there are some reports about friction drive employed to drive the telescopes. However friction drive has its own deficiencies, such as slippage and creepage. This report here describes the study on the friction drive finished in an experiment arranged by LAMOST project. It comprises three main parts. First, it introduces the experiment apparatus and proposes a new kind of measurement and adjustment mechanisms. Secondly, the report gives the analysis of friction drive characteristics theoretically, such as slippage, creepage and gives the results of corresponding experiments. The experiment shows that the lowest stable speed reaches 0.05″/s with precision of 0.009″(RMS), the preload has little influence on the drive precision in the case of constant velocity and the variable velocity when the angle acceleration is less than 5″/s^2 with close loop control and the creepage velocity of this experiment system is 1.47″ /s. Lastly, the analysis in the second section lists some measures to improve the precision and stability further. These measures have been actually conducted in the testing system and proved to be reliable.

Key words: large telescope, friction drive, ultra-low speed, slippage, creepage, critical speed

1. INTRODUCTION

The Large Sky Area Multi-object Fiber Spectroscopic Telescope(LAMOST), a national major scientific project in the process of construction in China, is a special reflecting Schmidt telescope with 4-meter aperture and 5° field of view. LAMOST consists of three parts: the reflecting Schmidt plate(M_A), the focal plane mechanism and the spherical primary mirror(M_B). The light from the observing celestial objects is reflected by Schmidt plate M_A, spherical mirror M_B and imaged on focal plane.

During the observation, three trackings are needed to get high quality image.They are azimuth tracking and altitude tracking of Schmidt plate and focal plane derotating. The tracking speed of the telescope is very slow(0～15″ /s), but the tracking accuracy is very high (0.4″)[1]. Friction drives are used for these motions of the telescope. Comparing to worm drive and gear drive, friction drive has some advantages, such as no significant short-term irregularities which is difficult to model and correct in the control system, free of backlash if the components are carefully designed and fabricated, and high precision tracking capabilities if outside disturbance, such as disbalanced torque and contaminants, are prevented from damaging the drive system. In this case, friction drive is widely and successfully used on some large astronomical telescopes. But friction drives do possess several inherent weaknesses, such as, high tracking precision requires high surface quality of the contact disks, extremely high pressure at the point of contact between the disks avoiding slippage, high precision bearing systems necessary to support the disks and capable of withstanding high loads. On the other hand, misalignment of the two disks axes will induce the slip motion between two disks and affect the tracking precision, what is more, the tracking and pointing velocity of LAMOST is very slow, in this case, stick-slip motion (creepage) is the main factor to affect the tracking and pointing accuracy. This paper presents the study on ultra-low speed characteristic and stability of friction drive. The experiment shows that the stable lowest speed reaches 0.05″/s with precision of 0.009″(RMS). Meanwhile, it analyses the mechanism theoretically of slippage and stick-slip motion which affects the precision of friction drive system.

*Guomin Wang, gmwang@nairc.ac.cn; phone 0086-025-85482232; fax 0086-025-85405562

Astronomical Structures and Mechanisms Technology, edited by
Joseph Antebi, Dietrich Lemke, Proceedings of SPIE Vol. 5495
(SPIE, Bellingham, WA, 2004) · 0277-786X/04/$15 · doi: 10.1117/12.550979

2. EXPERIMENTAL APPARATUS AND PROCEDURE

2.1 Overview

In early 2003, LAMOST project arranged the friction experiment to investigate the static and dynamic characteristics of friction drive system. A major goal of this effort was to develop a testing system to qualify the friction drive performance under ultra-low velocity operational condition. Another goal was to find out the factors which affect the accuracy and stability of friction drive and the measures to improve the drive precision. Fig. 1 shows the friction drive testing system and measuring system used in this study. It mainly consists of seven parts and some of them are described in detail in the following sections.

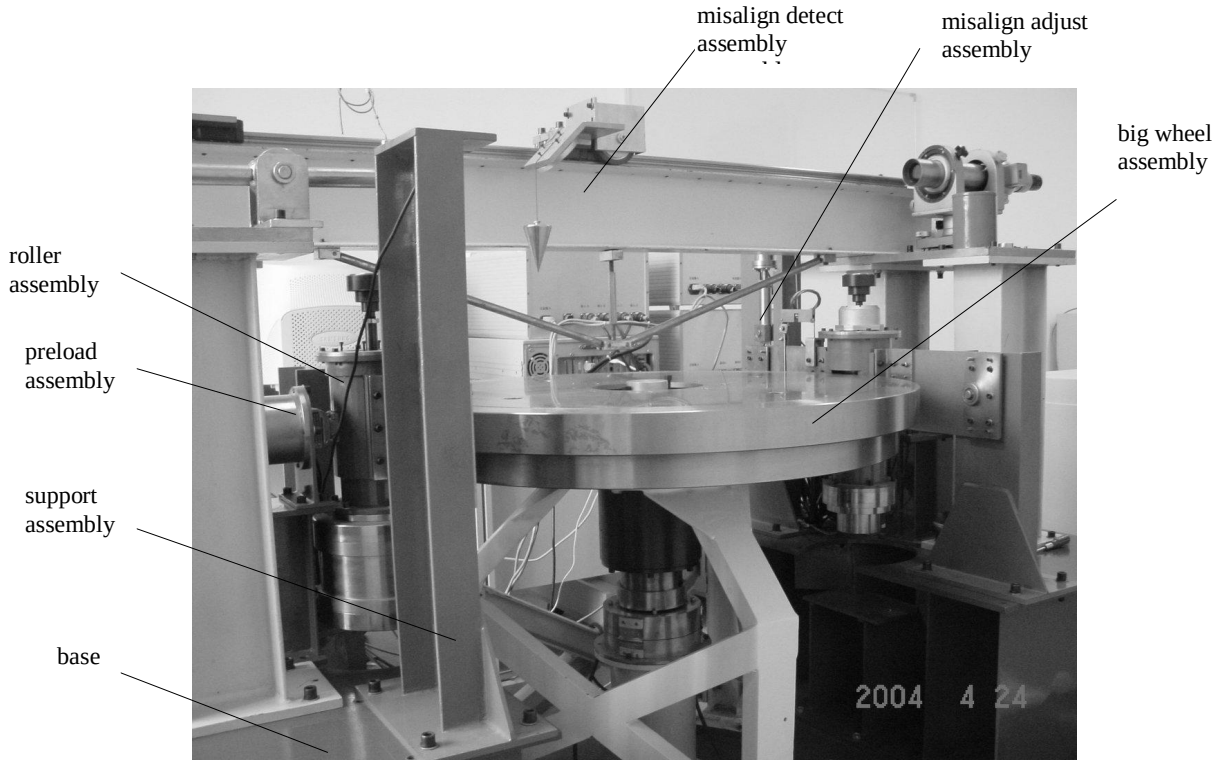

Fig.1 experiment apparatus picture

2.2 Roller assembly

There are two sets of roller mounting located on opposite sides of the big wheel (180-degrees apart) to minimize the eccentric caused by preload against the big wheel, just as the Fig. 1 shows. The friction rollers are 50mm thick and 50mm in diameter with a 0.01mm crown (corresponding to a crowning radius of 31250mm). The cylinders are made of an alloy of steel , heat-treated to a Rockwell C hardness of 55, that has a minimum yield strength of 120 Mpa. After the heat treatment, the rollers were finished with a grinder to remove the oxide layer so that the surface roughness Ra was measured as 0.4 μm. The contact (Hertzian) stress between the roller and wheel should be kept at an acceptably low level to avoid damaging the rollers while maintaining sufficient friction force. The length of contacting cylinders is 50mm. Assuming a steel-to-steel coefficient of friction of 0.11 and a contact force of 17.45 N per sector, the maximum drive torque is 0.8 N-m. According to the contact stress fomula, the maximum contact stress is 11.87 Mpa.

The rollers are mounted in the roller housing through angle-contact bearings and the roller housing is supported by two elastic plate made of spring steel. The stiffness of the elastic plate in the tangential direction is 1.85×10^4Kg/mm and

32.5Kg/mm in the normal direction. This allows the roller assembly to be pressed to the wheel surface to compensate for the surface runout of the big wheel. The torque motor-tachometer unit is in line with the drive shaft by use of a high stiffness coupler. In order to measure the skew angle of the misalignment between the axes of roller and wheel, two reflect mirrors are put on the top of the roller units mounted on-axis. Meanwhile, a high resolution optical incremental encoder (Heidenhain RON-225, 9000 lines on disc) is directly mounted to the roller axle for detecting slippage at the junction between the roller cylinder and big wheel.

2.3 Big wheel

The big wheel, 1000mm in diameter and 60mm thick made of bearing steel, is supported by three posts through ball bearings and thrust bearing just as shown in Fig. 1. The surface roughness Ra was measured as 0.4 μm, and the surface hardness was measured as Rockwell C hardness of 58. A high-precision, high-accuracy optical incremental encoder (Heidenhain RON-905, 36000 lines on disc, with 4096-fold increase in resolution) is directly coupled to the wheel axis to measure the position and feed back to the drive control system. The resolution of the encoder is 0.008 arc-seconds. Comparing to the off-axis coupling which can enhance the resolution, the on-axis coupling improves the repeatability and minimizes inaccuracies associated with friction roller driven encoder sysems. Just as the rollers, a reflect mirror is coupled to the wheel on-axis to measure the skew angle of the misalignment between the axes of roller and wheel.

2.4 Measure and adjustment assembly

Theoretically, the axes of roller and big wheel should be parallel to each other in spacial, that is to say, the roller should be adjusted so well that its axis of rotation is parallel to that of the surface on which it is rolling in all directions. In practical, it is hard to do so and then there are two kind of skew angle. One kind of skew angle is along the radial direction, and another one is in the tangential direction, just as Fig. 2 shows. Because the roller is supported by elastic plate, the skew angle in radial direction can be eliminated under the enough preload, but it does not work for the skew angle in tangential. If the roller is misaligned in tangential, this will generate an axial motion of the roller which increases as the roller rotates, just as twist-roller friction drive. This axial motion will be resisted by the roller bearings, and will give rise to an axial back force. When this force exceeds the frictional force between the contact surface, a elastic slip will occur. This will induce the uneven motion and introduce sharp errors in the control system. What is more, the roller misalignment may also cause premature wear on the disks and damage to the roller, the wheel and its bearings. The relationship between axial displacement S and skew angle θ is followed as: $S = \pi \times D \times tg\theta$ (D: the diameter of roller). For the 50mm roller in the experiment, a 30 arc-second skew misalignment will result in an implied axial displacement of 23 micron per roller revolution.

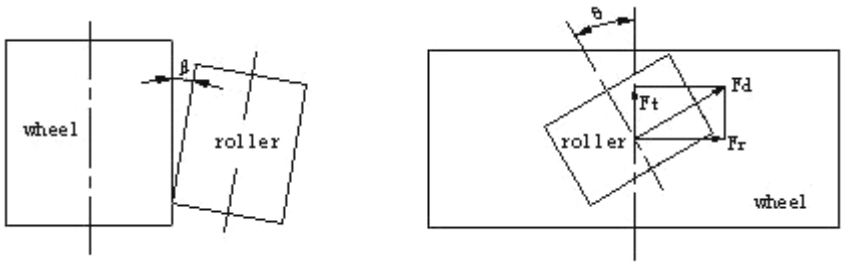

Fig.2 schematic diagram of skew angle

The measure mechanism of skew angle is shown in Fig. 3. It utilizes autocollimation to detect the skew angle. Three plate reflection mirrors are put on the top of axles of contact disks respectively. The errors caused by mirrors mounting is about 1.77 arc-second. There is a plate reflection mirror mounted on the cart with the 45° angle to the horizon. The cart is mounted on the high precision ball screw guide supported by I-beam whose stiffness is 1852 Kg/mm. With the help of autocollimation, the relative skew angle between rollers and wheel can be detected.

After detecting the relative skew angle, an adjust mechanism is used to revise the skew angle, shown in Fig. 4. The best situation is that the rotate axes of roller and wheel are parallel to each other, that is to say, the skew angle equals to zero. During the adjust operation, the axis of big wheel is regarded as the benchmark. The rollers' axes are adjusted to be parallel to the axis of the big wheel by means of the adjust mechanism. Just as described in section 2.2, the roller is supported by two elastic plates and formed a whole structure, we call it roller unit. The roller unit can rotate round a

pivot which is on one end of it. Another end of the roller unit is connected to the support post with the ball screw, as shown in Fig. 4. With the help of ball screw, the roller unit can be driven to rotate round the pivot.

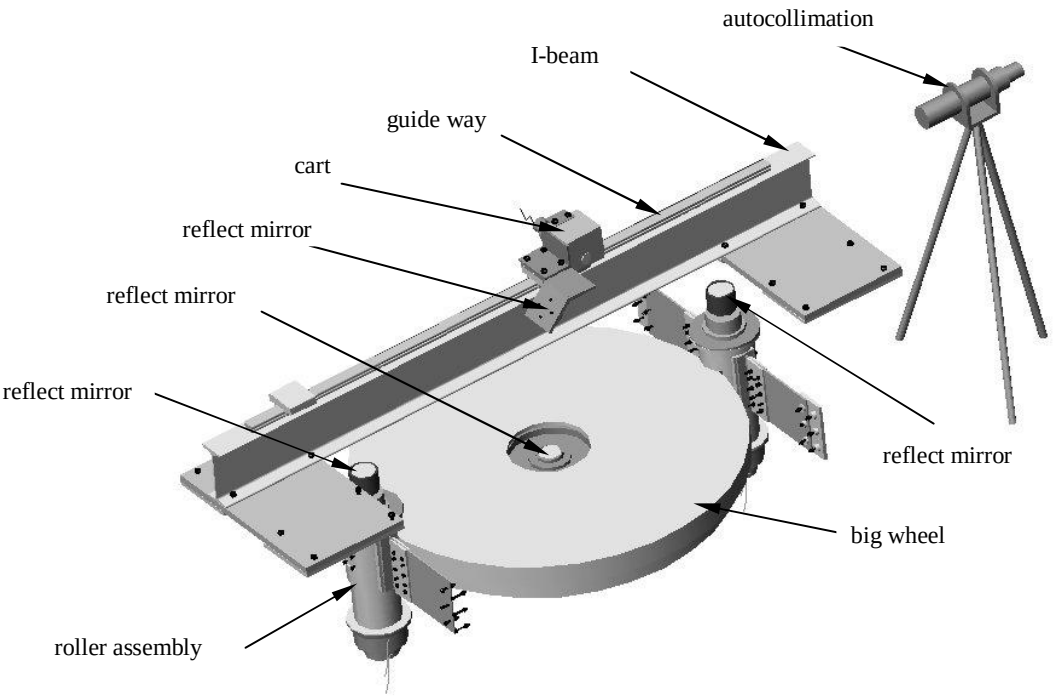

Fig.3 skew angle measurement assembly

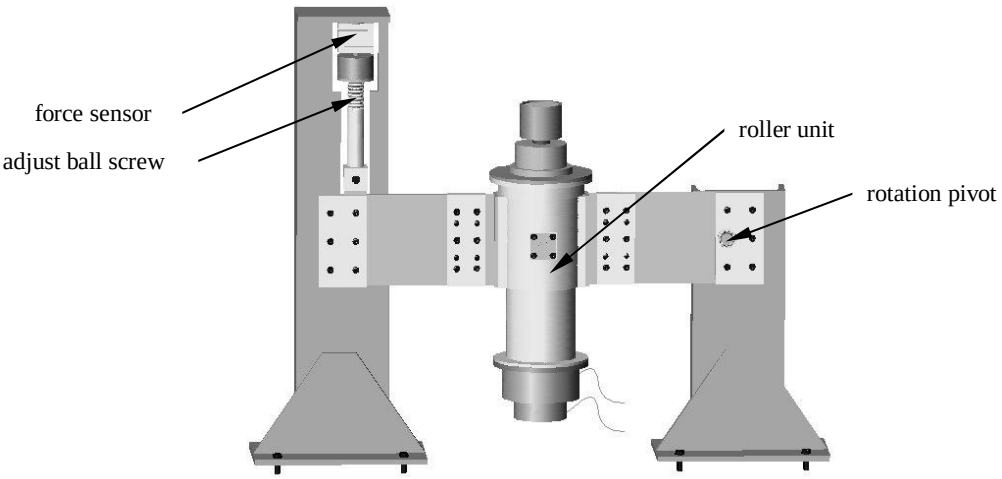

Fig.4 skew angle adjustment assembly

Since friction drives use contact friction to transmit the necessary drive power and torque between the driving and driven element, the cylindrical elements must be pressed together with sufficient force to maintain consistent drive between the roller and wheel with the lowest amount of slip under normal operation. On the other hand, the force must be low enough to maintain a safe level of contact (Hertzian) stress. The safe upper limit of preload can be got by calculating a suitable

contact stress value. The lower limit of preload is the critical load under which the slippage does not occur. One of the goals of this experiment is to find the relationship between the preload and drive precision. The preload is controlled by a compression spring, mounted in a housing with an adjustable screw device, that allows various spring loads to be applied on the roller. The ball screw is driven by a DC motor. Various spring preload is measured by a force sensor.

2.5 Control system

The control system consists of DC servomotor, tachometer, position feedback device, servo amplier and controller. The position controller calculate the error signal based on the position command and position feedback from increment encoder and send it to the velocity controller through D/A converter. The velocity controller computer the control signal according to the velocity error between the reference velocity and the actual tachometer readings and send the control signal to current control loop. The current control loop restrain the vibration of torque.

In order to get ultra-low velocity, a position control loop is added to the velocity control loop. This is different from traditional velocity control system. The position control loop will help to reduce the ripple of velocity. So the position control, velocity control and current control are cascade. PID algorithm is adopted in the system. The current controller and velocity controller are regulated to Type II system. In the position controller, the differentiator is added to reduce the influence of drive chain.

3. EXPERIMENTAL RESULTS AND DISCUSSION

3.1 Ultra-low velocity motion (constant velocity motion)

The lowest stable velocity in the experiment is 50 marcsec/sec and the corresponding precision is 9 marcsec RMS. The motion precision in different velocity are presented in table1. The values in the table are the mean of ten times.

Table 1 precision versus velocity

velocity (″/s)	0.05	0.1	0.2	0.5	1	5
precision RMS (″)	0.0090	0.0087	0.0083	0.0124	0.0139	0.0416
precision P-V (″)	0.0856	0.0873	0.0889	0.1612	0.2115	0.3219
velocity (″/s)	10	15	30	60	90	120
precision RMS (″)	0.1058	0.1578	0.2546	0.5138	0.8145	1.267
precision P-V(″)	0.8314	1.2094	1.7572	4.5357	5.6373	7.1086

According to table 1, the relationship between drive precision and velocity is showed in the Fig. 5.

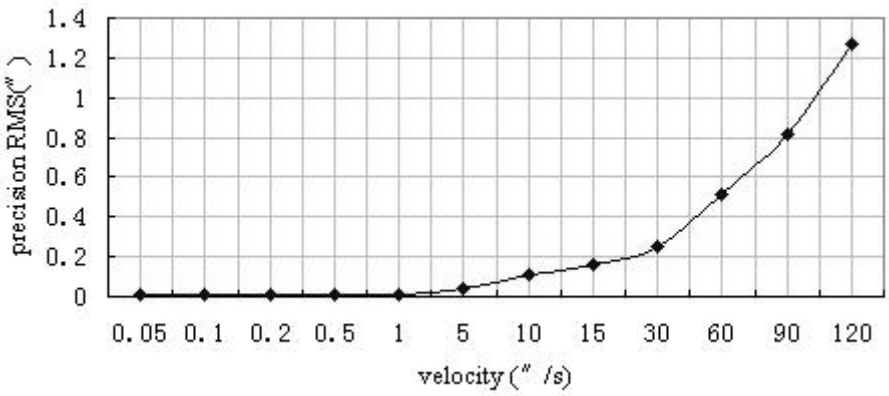

Fig.5 drive precision versus different velocity

It is easy to see from the Fig. 5 that the drive precision decreases with the velocity increasing and the variety is very large. Fig. 6 and Fig. 7 show the position error curves of 0.05″/s and 0.1″/s.

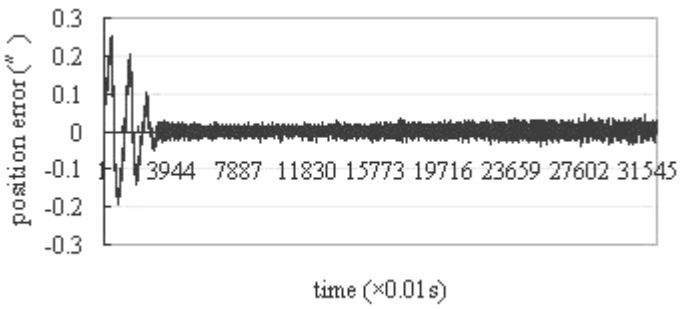

Fig.6 position error curve (0.05″ /s)

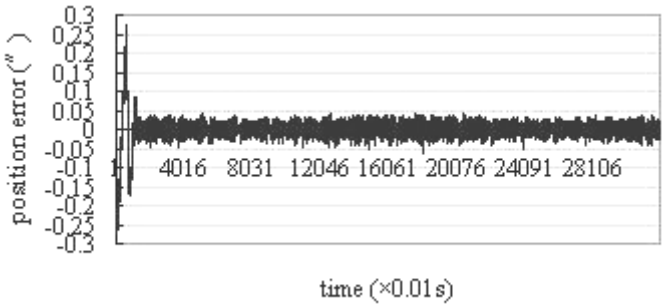

Fig.7 position error curve (0.1″ /s)

3.2 Relationship between precision and preload

Just as mentioned in section 2.4, one of the goals of this experiment is to find the relationship between the precision and preload. Typical results for the relationship between precision and preload in constant velocity and variable velocity are presented in Table 2 and Table 3 respectivelly and the corresponding curves are shown in Fig. 8 and Fig. 9. The values in these table are the mean of ten times.

Table 2 relationship between precision and preload (constant velocity)

P \ V / F	0.5	1	5	10	20	30
50	0.0105	0.011	0.0128	0.0623	0.1819	0.3363
100	0.0114	0.0153	0.0155	0.0864	0.2227	0.3815
200	0.0102	0.0158	0.0134	0.0937	0.1820	0.3576
300	0.0099	0.0149	0.0152	0.064	0.1917	0.3323
400	0.0088	0.0136	0.0143	0.0875	0.2399	0.4518
500	0.0101	0.0135	0.0141	0.0957	0.2387	0.3575

note: V-velocity (″ / s) P-precision rms (″) F-preload (N)

Table 3 relationship between precision and preload (variable velocity)

F \ P \ β	0.5	1	5	10	30	60
25	0.0607	0.1052	0.4651	0.8439	2.4713	4.5748
50	0.0594	0.0961	0.4692	0.8419	2.4028	4.3668
100	0.0564	0.0939	0.4589	0.8390	2.3889	4.5825
200	0.0572	0.0948	0.4277	0.8560	2.3835	4.3013
300	0.0571	0.0974	0.4143	0.8501	2.3638	4.2376
400	0.0590	0.0963	0.4109	0.8407	2.2900	4.2254
500	0.0569	0.0954	0.4324	0.8404	2.3082	4.2090

note: β-acceleration (″ / s ^{2}) P-precision rms (″) F-preload (N) A=180″

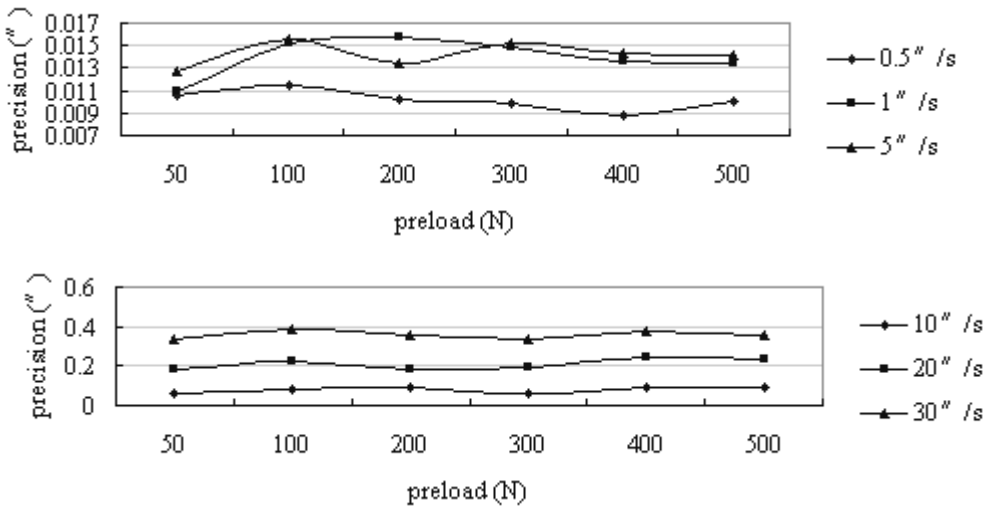

Fig.8 precision versus preload (constant velocity)

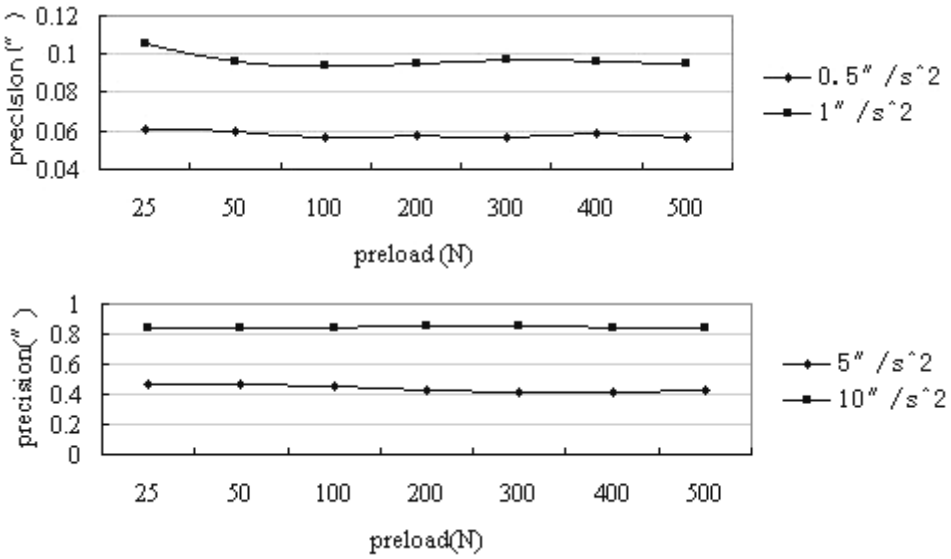

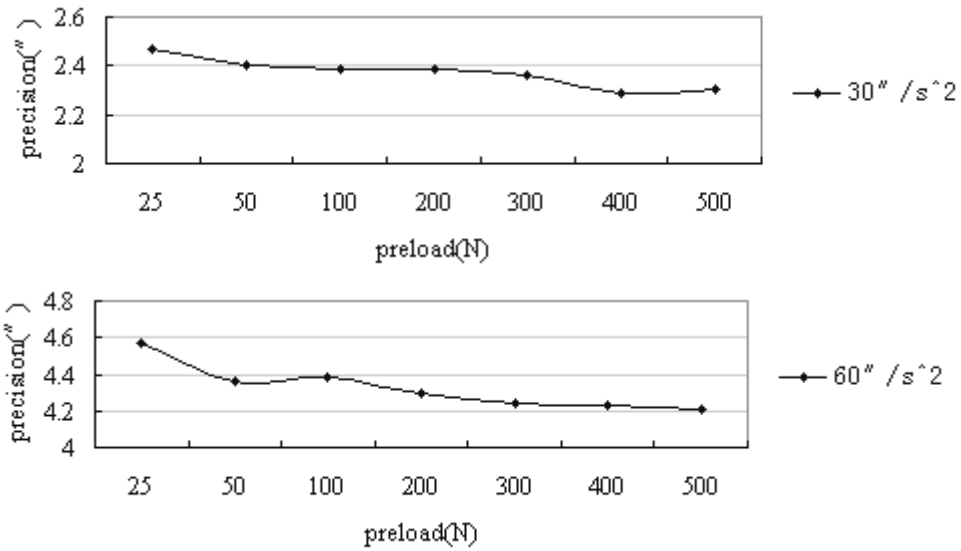

Fig.9 precision versus preload (variable velocity)

It can be seen from the results that the preload has little impact on the drive precision in the case of constant velocity and the variable velocity when the angle acceleration is less than 5″ /s^2. But when the angle acceleration exceeds 10″ /s^2, the preload has much impact on the precision. The precision varies from 4.6″ to 4.2″ with the preload increasing from 25N to 500N under the acceleration 60″ /s^2. On the other hand, it can be seen from the data that the relationship between preload and precision is not linear. Too large preload does not work on the improving of precision. The results show that the optimum preload for 30″ /s^2 and 60″ /s^2 is about 400N.

3.3 Analysis of stick-slip motion in ultra-low velocity

There are several interesting properties observed in systems with friction that do not respond instantaneously to a change of velocity. Examples of these includes: stick-slip motion, pre-sliding displacement, Dahl effect and frictional lag. Stick-slip motion is the major factor which can seriously degrade the properties of ultra low speed motion. It is the phenomenon of unsteady rotation, consisting of subsequent stick- and rotate-phase, caused by a decreasing friction force with increasing relative speed in combination with elasticity of the mechanical system. The phenomenon is explained in detail in several publications. Most of them are the research about the reciprocating friction drive system. However, the research about the ultra low speed rotation and its properties analysis are seldom to read on any reports. In the following section, the stick-slip characteristics of ultra low rotation is analysed from the view of dynamic and kinetic.

The drive system of telescope consists of different axles. The driven wheel should rotate in corresponding constant velocity when the motor rotates in the constant velocity. But due to the variation of friction force in the bearings and drive devices, the driven wheel rotates in a unsteady situation. Huang[2] investigated the stability characteristics of rotation in ultra low velocity. Figure 10 is a typical rotation model. Motor drives the wheel through the drive chain. The wheel has moment of inertia and damping, and the stiffness of the drive chain is K, so the system of friction drive system of Fig. 10 could be modeled as Fig. 11.

Assuming the friction torque of the system is M_f (static friction torque is M_{fs}, kinematic friction torque is M_{fd}), and the load torque is M_w, the drive torque is M_d. In the critical condition(M_d=M_{fs}+M_w), the initial rotate angle α_0 is:

$$\alpha_0 = \frac{M_d}{K} = \frac{M_{fs} + M_W}{K} \qquad (1)$$

when M_d>M_{fs}+M_w, the wheel begin to rotate, and the M_{fs} decreases to M_{fd}. When the wheel rotate in the constant velocity ω_1, the corresponding rotation equation is:

$$K(\alpha_0 + \omega_1 t + \beta) - (M_{fd} + M_w + \Delta M_w) - r\frac{d\beta}{dt} = I\frac{d^2\beta}{dt^2} \qquad (2)$$

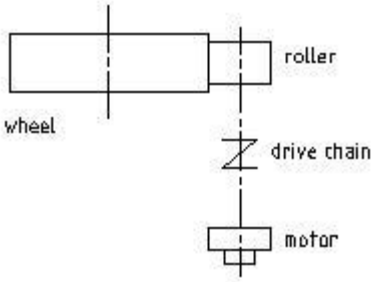

Fig.10 schematic diagram of friction drive

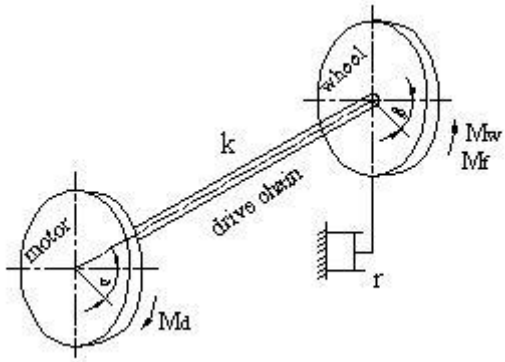

Fig.11 model of friction drive

return the α_0 to this equation, then

$$\ddot{\beta} + 2\xi\omega_n \dot{\beta} + \omega_n^2 \beta = \omega_n^2 \omega_1 t + \frac{\Delta M}{I} \qquad (3)$$

where: ξ is damping coefficient $\xi = \frac{r}{2\sqrt{IK}}$ ω_n: natural frequency $\omega_n = \sqrt{\frac{K}{I}}$

$\triangle M$ is variation of system torque, $\triangle M = M_{fs} - M_{fd} - \triangle M_w$

the answer of the equation (3) is (assuming $\xi << 1$):

$$\beta = e^{-\xi\omega_n t}\left(B_1 \sin\omega_n t + B_2 \cos\omega_n t\right) + \omega_1 t - \frac{r\omega_1}{K} + \frac{\Delta M}{K} \qquad (4)$$

according to the equation (4), the velocity and acceleration can be got as followings:

$$\dot{\beta} = \omega_1 \left\{ 1 - e^{-\xi\omega_n t}\left[(\xi - A)\sin\omega_n t + \cos\omega_n t\right] \right\}$$

$$\ddot{\beta} = \omega_1 \omega_n e^{-\xi\omega_n t}\left[(1 - A\xi)\sin\omega_n t + A\cos\omega_n t\right]$$

The premise of steady rotation is that velocity should be above zero and the acceleration equals to zero. In this case, we can get the critical velocity ω_c:

$$\omega_c = \frac{\Delta M}{A_c\sqrt{KI}} = \frac{M_{fs} - M_{fd} + \Delta M_w}{A_c\sqrt{KI}}$$

among the equation, A_c is the coefficient of steady motion. It equals to $(4\pi\xi)^{1/2}$ approximately. So the critical velocity is :

$$\omega_c = \frac{\Delta M}{\sqrt{4\pi\xi KI}} \qquad (5)$$

Among the critical speed formula, ΔM is the variation of the friction torque, ξ is the damping coefficient, K is the stiffness of the drive system and I is the moment of inertia of the rotation parts. So if we can measure these parameters, we can get the critical velocity of the system. We will calculate the critical velocity of the experiment system.

The damping coefficient of the system is 0.025 got from the design manual, and the moment of inertia of the system is 74.54 kg-m^2 derived using finite element analysis. For the parameters ΔM and K, we got them through measure because there are much difference between the actual value and calculation value. With the help of the torque sensor, we got the ΔM. The ΔM of this system is 0.15 N-m. The stiffness K is the rotate angle variation versus the corresponding torque variation. So we record the various angle under the different torque and measure the stiffness of the system. The stiffness of the experiment system is 1.89e7 N-m/rad. Acccording to these parameters, the critical velocity of the experiment system is 1.47 arcsecond/sec. The stick-slip motion curves of 0.05″ /s is shown in Fig. 12.

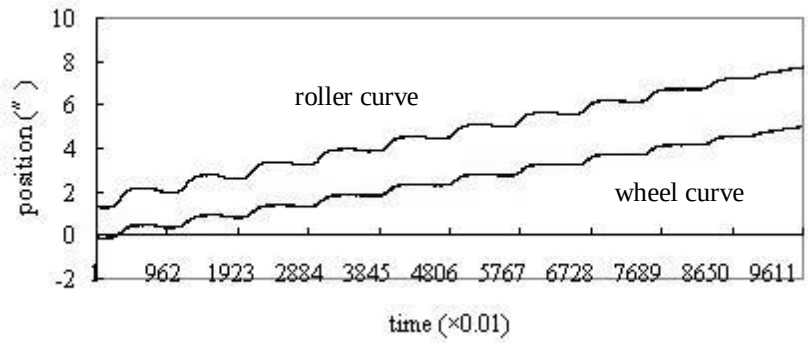

Fig.12 stick-slip motion of 0.05″ /s

4. CONCLUSIONS AND COMMENTS

(1) Friction drive can get high precision under ultra low velocity. The steady ultra low speed is 0.05″ /s in the experiment and the corresponding precision is 0.009″ RMS.

(2) The roller mount has to be very stable in the tangential direction and be flexible in the radial direction to compensate the runout of the big wheel. The axial movement of the roller is not allowed.

(3) In order to get high precision of friction drive, the axes of roller and wheel should be adjusted to parallel to each other to avoide slippage. In the experiment, the resolution of the autocollimation is 4 arcsecond, so the accuracy of the parallel between the axes is about 30 arcseconds.

(4) Keeping the contact surface dry and clean are the premise of getting high performance of friction drive.

(5) The key is that the pressure between the wheel and roller must be high enough to prevent any slipping but low enough to prevent damage to the surface. The best results are in a proper preload range, and the preload should be adjustable and calibratable.

(6) The preload has little influence on the drive precision in the case of constant velocity and the variable velocity when the angle acceleration is less than 5″ /s^2 with close loop control. But when the angle acceleration exceeds 10″ /s^2, the preload has much impact on the precision. The precision varies from 4.6″ to 4.2″ with the preload increasing from 25N to 500N under the acceleration 60″ /s^2. On the other hand, too lagre preload does not work on the improving of precision.

(7) The stick-slip motion is the main factor which affects the low speed characteristics of friction drive. Various drive system has its own critical speed over which the stick-slip phenomena does not occur. To this experiment system, the critical speed is 1.47 arcsecond/sec. Theoretically speeking, because of the damping of the system, the stick-slip phenomena will eliminate as the time is going. Just as the critical velocity formula shows, high stiffness and low difference between static and kinetic torque are the good ways to prevent the stick-slip phenomena.

ACKNOWLEDGEMENTS

The authors would like to express their appreciation to the LAMOST project for the financial support and to thank the LAMOST staff, in particular these technicians who took part in the mounting and calibration the experiment apparatus.

REFERENCES

1. Yao Zheng-qiu，Li Guo-ping，“The Tracking System of LAMOST Telescope”，*SPIE* Vol.3352，P560-571
2. Huang Qisheng, “The Stability Research of Rotation in Ultra low velocity”, *Mechanical Design*(1998), P7-8
3. Robert Kibrick，Steve Allen，“Method for measuring and reducing slippage of friction rollers empolyed in off-axis coupling of position encoders to telescopes”，*SPIE* Vol. 1236 IV 1990，P777-789
4. P. De Baets, J. Degrieck, F. Van De Velde, A. P. Van Peteghem, “Experimental verification of the mechanisms causing stick-slip motion originating from relative deceleration”, *Wear* 243 (2000) 48-59
5. Wang Jian-li，Li-zhen，Liu Hai-ning，“Slippage calculation in friction drive design”，*Machine Design and Research*，1998 No.4，P49-50